Fluorescence Studies of the Binding of Anionic Derivatives of Pyrene and Fluorescein to Cationic Polyelectrolytes in Aqueous Solution

Frank Caruso,*,† Edwin Donath,† Helmuth Möhwald,† and Radostina Georgieva‡

Max Planck Institute of Colloids and Interfaces, Rudower Chaussee 5, D-12489 Berlin, Germany, and Department of Biophysics, Thrakian University, Stara Zagora, Bulgaria

Received April 7, 1998; Revised Manuscript Received July 10, 1998

ABSTRACT: The electrostatic binding of the anionic probes pyrenetetrasulfonic acid (4-PSA) and 6-carboxyfluorescein (6-CF) to poly(allylamine hydrochloride) (PAH), poly(diallyldimethylammonium chloride) (PDADMAC), and DADMAC−acrylamide (AAM) copolymers in aqueous solution has been investigated by fluorescence spectroscopy. Binding of the probes to the polyelectrolytes causes changes in their fluorescence emission and excitation spectra, which allows conclusions to be drawn about their binding mechanisms. 4-PSA forms excimers in the presence of PAH or PDADMAC, whereas the presence of polyelectrolyte in 6-CF solutions induces fluorescence self-quenching of 6-CF. Through measurement of the 4-PSA excimer to monomer emission ratio (I_E/I_M) as a function of 4-PSA concentration or through evaluation of the minima in the 6-CF fluorescence concentration curves in the presence of polyelectrolyte, the amount of probe electrostatically bound to the polyelectrolytes and hence the binding stoichiometry at saturation binding conditions were determined. Binding experiments using copolymers of DADMAC and AAM with various charge densities showed that the DADMAC charge density over the range 21−100 mol % had little effect on the binding stoichiometry of 4-PSA but a marked influence on that of 6-CF. The data obtained are evaluated using a theoretical model based on probability considerations in order to examine the role of polyelectrolyte flexibility and binding site topology on the probe−polyelectrolyte interactions.

Introduction

Fluorescent molecules have been widely used to probe the microenvironments of organized host media ranging from micelles and microemulsions to bilayers and monolayers.[1] There has also been much interest surrounding the use of fluorescent probes to characterize polyelectrolytes, polyelectrolyte complexes, and hydrogels.[2] One of the most commonly used probes is pyrene, which is particularly attractive because of its relatively long fluorescence lifetime in the excited state, its ability to measure the polarity of its microenvironment via the intensities of the first and third vibronic bands of the monomer emission, and its tendency to form excimers with a distinct fluorescence.[1,2] Unsubstituted pyrene and polyelectrolytes with pyrene covalently attached are often employed to investigate the properties of polymers in solution.[1−3]

However, ionic derivatives of pyrenes have been used to a lesser extent.[4−9] The binding of ionic pyrene probes,[4−9] as well as (arylmethyl)ammonium probes,[10,11] to polyelectrolytes of the opposite charge, has recently been demonstrated. Electrostatic attraction between the oppositely charged probes and polyelectrolytes is the driving force for the binding.[7−9] Binding is manifested by quenching of the monomer emission, the appearance of excimer emission, and changes in the probe fluorescence excitation and absorption spectra. Although these studies have employed various polyelectrolytes, a systematic investigation of polyelectrolyte charge density on probe fluorescence and binding was not undertaken, nor was the effect of polyelectrolyte flexibility on probe binding examined. In addition, the binding stoichiometry of the probe to the polyelectrolytes was not quantitatively assessed in those investigations.

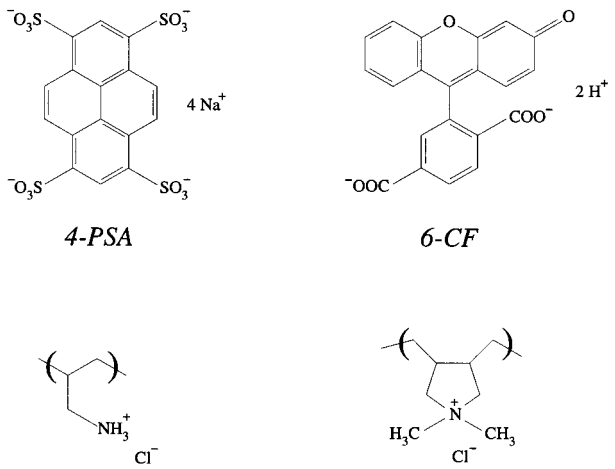

Figure 1. Structures of the fluorescent probes and the polyelectrolytes used in this study.

In this work, we examine the binding of two anionic probes, pyrenetetrasulfonic acid (4-PSA) and 6-carboxyfluorescein (6-CF), to poly(allylamine hydrochloride) (PAH) and poly(diallyldimethylammonium chloride) (PDADMAC) in aqueous solution. 6-CF was chosen because of its high absorptivity and high fluorescence quantum yield, as well as its self-quenching capacity via fluorescein-to-fluorescein excited-state energy transfer.[12,13] The self-quenching behavior of 6-CF can be exploited to investigate its binding to the polyelectrolytes. The structures of the probe molecules and the polyelectrolytes used are shown in Figure 1. PAH is a more flexible polyelectrolyte than PDADMAC, and therefore by employment of these polyelectrolytes, the

* To whom correspondence should be addressed. Fax: +49 30 6392 3102. E-mail: caruso@mpikg.fta-berlin.de.
† Max Planck Institute of Colloids and Interfaces.
‡ Thrakian University.

10.1021/ma980538d CCC: $15.00
Published on Web 10/02/1998

importance of flexibility on the mutual interaction between the probe and the polyelectrolyte can be assessed. The effect of charge density on the extent of probe binding is also examined in this work by using DADMAC−acrylamide (AAM) random copolymers with DADMAC contents of 8, 21, 35, 47, 58, and 73 mol %. The use of the copolymers permits investigation of the required topology of the binding sites, as well as determination of the binding stoichiometry as a function of DADMAC content in the copolymer.

The binding data obtained are evaluated using a theoretical model based on probability considerations employing combinatorial mathematics to arrive at a better understanding of probe binding to polyelectrolytes in aqueous solution. There are only a few existing models for describing the binding of probes to polymer systems. An early model proposed by Becker et al.[9] for the association of probes and polyelectrolytes allows calculation of binding constants but is not sufficient to explain the binding stoichiometry because it does not take into account the topology of binding sites in the polyelectrolytes. Its use is therefore limited, and it cannot be applied to copolymer systems. Reid and Soutar[14,15] reported that a linear dependence of the excimer to monomer ratio with local probe concentration can be predicted from kinetic models for copolymer systems interacting with probe molecules. Application of these models, however, requires detailed knowledge of energy migration parameters (rate constants of internal conversion, intersystem crossing, fluorescence, deactivation, and excimer formation) for the photoprocesses. The theoretical model proposed in this work has the advantage that it takes into account the arrangement of binding sites in describing the probe binding behavior, therefore making it applicable to a wide range of polymer systems. Its application is also *not* restricted to excimer-forming probe molecules in polymer systems.

The motivation for the current work was two-fold: first, to examine the effect of polyelectrolyte flexibility and binding site topology on the electrostatic binding of the probe molecules in solution and, second, to extend this work to investigate the nature of the electrostatic interactions between polyelectrolytes in ultrathin multilayer films. Polyelectrolytes have greatly impacted the area of thin film fabrication since the recent introduction of the layer-by-layer self-assembly technique,[16] with PAH and PDADMAC being two of the most frequently used polyelectrolytes in the construction of such films.[16]

Experimental Section

Materials. Poly(allylamine hydrochloride) (PAH; M_w = 8000−11 000) and poly(diallyldimethylammonium chloride) (PDADMAC; M_w > 350 000) were obtained from Aldrich. Random copolymers of DADMAC and acrylamide (DADMAC−AAM) with DADMAC contents of 8, 21, 35, 47, 58, and 73 mol % were kindly donated by H. Dautzenberg (Max Planck Institute of Colloids and Interfaces, Teltow-Seehof, Germany). (Details on the synthesis and characterization of these copolymers can be found elsewhere.[17]) 1,3,6,8-Pyrenetetrasulfonic acid tetrasodium salt (4-PSA) was purchased from Molecular Probes, Eugene, OR. 6-Carboxyfluorescein (6-CF) was obtained from Sigma. All polyelectrolytes and probes were used as received. The water used in all experiments was prepared in a three-stage Millipore Milli-Q Plus 185 purification system and had a resistivity higher than 18.2 MΩ cm.

Fluorescence and Absorption Measurements. Fluorescence spectra were obtained using a Spex Fluorolog 1680 spectrometer. Both excitation and emission bandwidths were set at 1.0 nm. Absorption spectra were obtained using a Varian Cary-3 UV−visible spectrophotometer. The pH of the stock 1 mM 6-CF solution was 6.0 ± 0.1. Experiments were performed either by adding polyelectrolyte to a solution containing probe or by adding probe to a polyelectrolyte solution. Both methods yielded identical spectra for solutions containing the same ratio of probe to polyelectrolyte amount. All solutions were stirred for 1 min prior to recording of the spectra. All measurements were performed on air-equilibrated solutions at 25 °C.

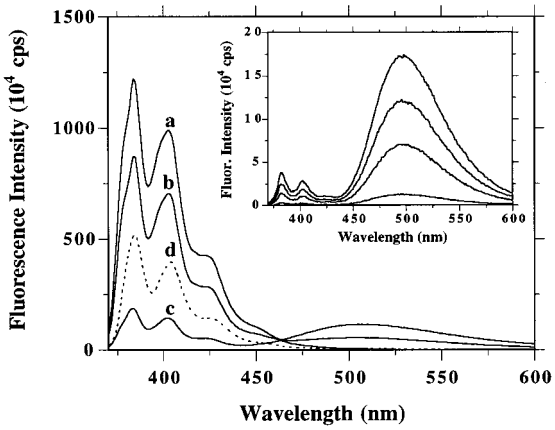

Figure 2. Fluorescence spectra of 5×10^{-6} M 4-PSA in the absence and presence of PAH. [PAH]: (a) 0; (b) 0.66; (c) 1.66; (d) 2500 μg mL^{-1}. Excitation wavelength = 350 nm. The inset shows the fluorescence spectra of 4-PSA added to 5 μg mL^{-1} PAH. Spectra (from bottom to top): 0.07, 0.40, 0.72, and 1.0 μM 4-PSA. Excitation wavelength = 350 nm.

Results

Binding of 4-PSA and 6-CF to PAH. Figure 2 displays the fluorescence spectra of 5×10^{-6} M 4-PSA in aqueous solution in the absence (a) and presence (b−d) of PAH. 4-PSA in water exhibits only the characteristic monomer emission (I_M), with maxima at 384 and 403 nm and a shoulder at 424 nm. The presence of PAH (up to a concentration of 2.3 μg mL^{-1}) causes a systematic reduction in the monomer intensity and induces typical pyrene excimer formation (I_E), seen as a broad, structureless band centered around 500 nm (b and c). At 2.3 μg mL^{-1} PAH there is a decrease of more than 99.5% of the original monomer fluorescence intensity (spectra not shown). At higher PAH concentrations the monomer fluorescence intensity increases, reaching a maximum at 2.5 mg mL^{-1} PAH (d). This increase in monomer intensity is accompanied by the disappearance of the excimer emission. The decrease in the 4-PSA monomer fluorescence intensity observed for the lower PAH concentrations (0.6−2.3 μg mL^{-1}) can be explained by sequestering of 4-PSA by the polyelectrolyte, resulting in an increase in the local concentration of the probe molecules along the polymer chain and promoting excimer formation and fluorescence quenching. As the polyelectrolyte concentration is further increased, the probe molecules can redistribute along the polymer chain due to the increased number of binding sites available in the polymer. This is evidenced as an increase in the monomer intensity since the degree of excimer formation is reduced. The inset of Figure 2 shows spectra in the probe−polyelectrolyte concentration region where the 4-PSA emission is predominantly due to excimer fluorescence. Identical spectra are obtained for solutions of a given concentration of probe and polyelectrolyte, regardless of whether the probe is

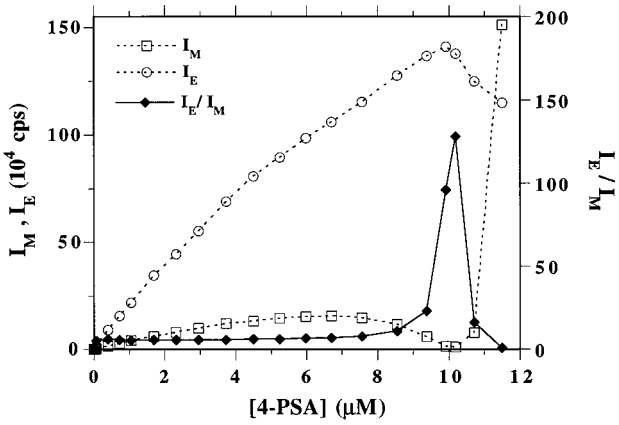

Figure 3. I_M (383 nm), I_E (495 nm), and I_E/I_M as a function of 4-PSA concentration for 4-PSA added to 5 μg mL^{-1} PAH. Excitation wavelength = 350 nm. The lines drawn through the experimental data are to guide the eye.

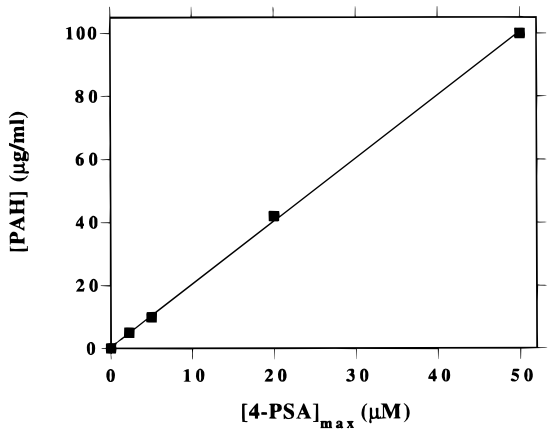

Figure 4. PAH solution concentration as a function of the concentration of 4-PSA bound to PAH at saturation binding.

added to a polyelectrolyte solution or the polyelectrolyte to a probe solution.

Figure 3 shows the dependence of 4-PSA I_M, I_E, and I_E/I_M on 4-PSA concentration at a PAH concentration of 5 μg mL^{-1}. I_E increases up to ca. 10 μM 4-PSA, whereas the maximum I_M occurs at ca. 7 μM 4-PSA. Above this concentration I_M steadily decreases until reaching a minimum value at a 4-PSA concentration corresponding to the maximum I_E. This decrease in I_M is attributed to a combination of excimer formation and self-quenching of 4-PSA as a result of its binding to PAH. At 4-PSA concentrations above 10 μM, a sharp increase in I_M is observed. This increase is ascribed to 4-PSA remaining in bulk solution since the polyelectrolyte binding sites are saturated with 4-PSA (see later). Curves similar to those shown in Figure 3 were obtained when the PAH concentration was varied between 2 and 100 μg mL^{-1}.

The maximum amount of 4-PSA bound to PAH (i.e., saturation binding, $[4\text{-PSA}]_{max}$) can be taken as that at which a maximum in I_E/I_M is observed or that just prior to a rapid increase in I_M (Figure 3). The monomer fluorescence intensity at this concentration (10 μM) is essentially zero, indicating that the amount of 4-PSA in free solution (i.e., unbound 4-PSA) is negligible. Figure 4 shows that there is a linear relationship between the concentration of PAH in solution and $[4\text{-PSA}]_{max}$. This suggests that a given stoichiometry exists for the binding of 4-PSA to PAH in solution.

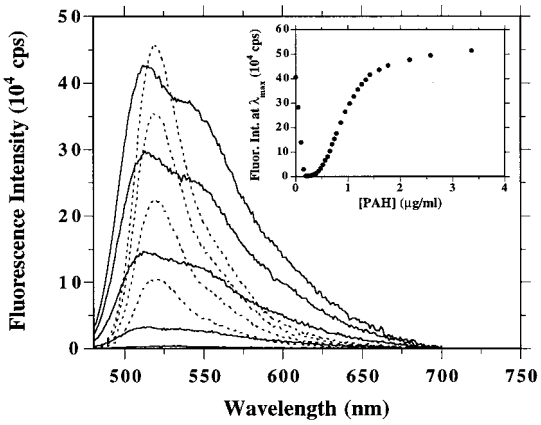

Figure 5. Fluorescence spectra of 5 × 10^{-7} M 6-CF in the absence and presence of PAH. Spectra (from top to bottom, solid line): 0, 0.05, 0.10, 0.15, and 0.20 μg mL^{-1} PAH. Spectra (from bottom to top, dashed line): 0.65, 0.87, 1.2, and 1.8 μg mL^{-1} PAH. Excitation wavelength = 450 nm. The inset shows the 6-CF fluorescence intensity at maximum wavelength as a function of PAH concentration.

Steady-state fluorescence excitation spectra for 4-PSA in the presence of PAH, obtained by excitation from 250 to 400 nm and monitoring of the emission at both 410 (monomer) and 495 (excimer) nm, showed that the spectrum monitored at the monomer fluorescence maximum of 410 nm is well-resolved, whereas the spectrum monitored at 495 nm is broadened and red-shifted by several nanometers relative to that of the monomer spectrum (spectra not shown). Similar shifts have been observed for other probe−polyelectrolyte systems and are indicative of polyelectrolyte-induced interaction of aromatic rings in the ground state of the probe.[5−9] Thus, the spectra obtained indicate that ground-state interactions of the pyrene moieties of 4-PSA occur when bound to PAH. Further evidence for this type of interaction is obtained from absorption measurements, which show a broadened and slightly red-shifted 4-PSA absorption spectrum in the presence of PAH, relative to that of 4-PSA with no added PAH.

The effect of PAH on the fluorescence spectrum of 5 × 10^{-7} M 6-CF is demonstrated in Figure 5. A noticeable red-shift in the 6-CF fluorescence maximum at 512 nm occurs with increasing PAH concentration: this maximum shifts from 512 nm (no PAH present) to 520 nm at the highest PAH concentrations. In addition, the shoulder observed in the 6-CF spectrum at about 540 nm, which is characteristic of free 6-CF in solution, disappears with increasing PAH concentration. This clearly demonstrates binding of 6-CF to PAH. In the presence of PAH, the 6-CF fluorescence intensity decreases due to fluorescence self-quenching, as a result of extraction of the probe from the aqueous domain to that of the polyion (Figure 5, inset). (6-CF self-quenching occurs via fluorescein-to-fluorescein excited-state energy transfer toward a nonfluorescent trap.[12,13]) Beyond the PAH concentration which causes essentially total quenching of 6-CF fluorescence and where saturation of the polyelectrolyte binding sites by the probe occurs, an increase in the fluorescence intensity is observed (Figure 5, inset). As discussed above for the 4-PSA/PAH system, this fluorescence increase can be explained by distribution of the 6-CF molecules over the larger number of available binding sites on the polyelectrolyte with increasing polyelectrolyte concentration, thereby reducing self-quenching.

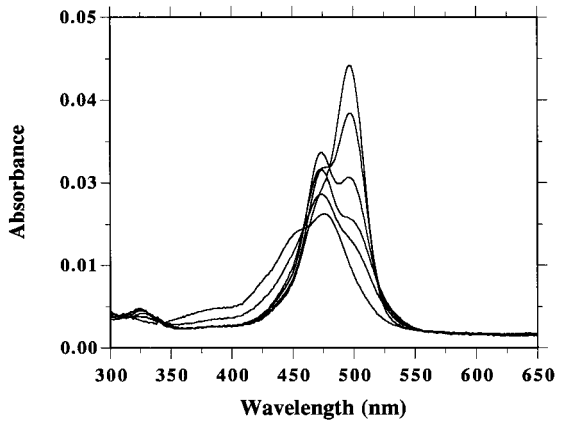

Figure 6. Absorption spectra of 5×10^{-7} M 6-CF in the absence and presence of PAH. Spectra (from bottom to top at 500 nm): 0, 0.10, 0.20, 0.43, 0.98, and 11.8 μg mL^{-1} PAH.

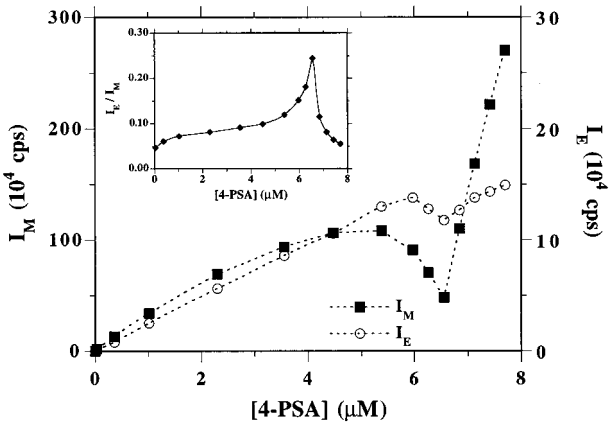

Figure 7. I_M (384 nm) and I_E (500 nm) as a function of 4-PSA concentration for the binding of 4-PSA to 5 μg mL^{-1} PDADMAC. The inset shows a plot of I_E/I_M versus 4-PSA concentration. Excitation wavelength = 350 nm. The lines drawn through the experimental data are to guide the eye.

The absorption spectra of 6-CF in the absence and presence of PAH are shown in Figure 6. The spectrum of 6-CF in water contains a major band at 475 nm. Upon addition of PAH, this band increases in intensity and a new band appears at 497 nm, which arises from the binding of 6-CF to PAH. The new band at 497 nm increases with increasing PAH concentration, replacing the 475 nm band at higher PAH concentrations. Similar shifts in absorption maxima have been reported for the interaction of anionic probes with various cationic polyelectrolytes.[7]

Binding of 4-PSA and 6-CF to PDADMAC and DADMAC−AAM Copolymers. Both monomer and excimer emission are observed for 4-PSA in the presence of PDADMAC in aqueous solution. The dependence of 4-PSA I_M and I_E on 4-PSA concentration for the binding of 4-PSA to PDADMAC are shown in Figure 7. A plot of I_E/I_M versus 4-PSA concentration is displayed in the inset. The value for I_E/I_M at maximum probe binding to PDADMAC is several orders of magnitude less than that obtained for 4-PSA in the presence of PAH (Figure 3). Although considerably more monomer fluorescence is observed for the 4-PSA/PDADMAC system than the 4-PSA/PAH system, the monomer intensity observed at maximum I_E/I_M is less than 1% of that observed for 4-PSA at this same concentration (where I_E/I_M is maximum) in the *absence* of polyelectrolyte. Thus, it can be concluded that the monomer fluorescence observed is due to bound 4-PSA. From these data it is clear that PAH in solution clearly facilitates excimer formation to a greater degree than PDADMAC, although the qualitative features of the data for 4-PSA binding to the two polyelectrolytes are similar.

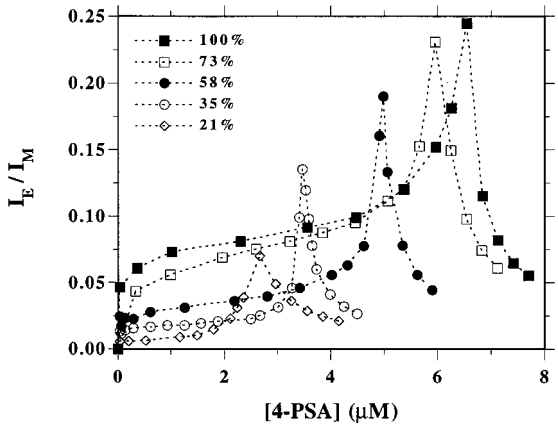

Figure 8. I_E/I_M as a function of 4-PSA concentration for the interaction of 4-PSA with 5 μg mL^{-1} DADMAC−AAM copolymers with various charge densities. The DADMAC contents in the copolymers are 21, 35, 58, and 73 mol %. The experimental data for the homopolymer (PDADMAC, 100%) are also shown. Excitation wavelength = 350 nm. The lines drawn through the experimental data are to guide the eye.

The effect of polymer charge density on the binding of 4-PSA was investigated by employment of DADMAC−AAM random copolymers with various DADMAC contents. The I_E/I_M versus 4-PSA concentration curves for 4-PSA with 5 μg mL^{-1} of copolymer in solution (Figure 8) demonstrate that the amount of 4-PSA bound is dependent on the DADMAC content in the copolymer. (The experimental data for the homopolymer, PDADMAC, are also shown.) The amount of excimer at a given total copolymer concentration decreases as the number of binding groups (DADMAC) in the polymer is reduced (data not shown). As the DADMAC content decreases in the copolymer, bound pyrene molecules are on average further apart. These observations provide further evidence that there is a stoichiometric interaction of 4-PSA with DADMAC. In contrast to the case for 4-PSA in the presence of PAH, fluorescence excitation spectra for 4-PSA in the presence of PDADMAC obtained by excitation from 250 to 400 nm and monitoring of the emission at 410 (monomer) and 495 (excimer) nm did not reveal ground-state interactions of 4-PSA (within the resolution of the experiments)—no noticeable broadening or red-shift in the spectra was observed.

The influence of the DADMAC−AAM copolymers with various charge densities on the fluorescence of 6-CF is demonstrated in Figure 9. Except for the 8 and 21 mol % DADMAC−AAM copolymers, the 6-CF fluorescence intensity first increases at low 6-CF concentrations (0−2.5 μM) (slope$_i$), then decreases at higher values, and once again increases as the 6-CF concentration is increased (slope$_f$). The nonmonotonic behavior is qualitatively understood as follows. At low 6-CF concentrations the fluorescence quantum yield is constant, causing the linear fluorescence intensity increase; 6-CF self-quenching then becomes dominant, and at higher concentrations the polyelectrolyte is saturated and the emission of the unbound probe is observed. Hence, the 6-CF concentration prior to the onset of the second intensity increase is taken to correspond to the approximate maximum amount of 6-CF bound to the

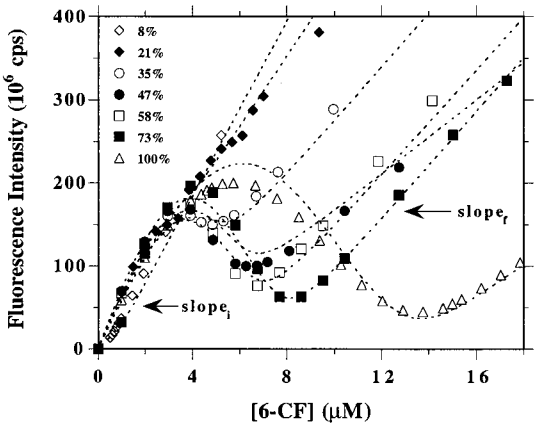

Figure 9. Fluorescence intensity (total area under spectrum from 480 to 620 nm) as a function of concentration for 6-CF in the presence of 5 μg mL^{-1} DADMAC−AAM copolymers with various charge densities. The DADMAC contents in the copolymers are 8, 21, 35, 47, 58, and 73 mol %. The experimental data for the homopolymer (PDADMAC, 100%) are also shown. Excitation wavelength = 450 nm. The total areas under the emission spectra were used instead of the maximum fluorescence values since the shape of the spectra were affected by resonance energy transfer. The curves are theoretical fits to the experimental data (see text for details). $K = 2.5 \times 10^7$ M^{-1}, $k_{di} = 0.18$, $k_{ri} = 2.25i^{-1}$ ($i \geq 3$). The initial (slope$_i$) and final (slope$_f$) fluorescence intensity slopes are also indicated.

copolymer. This is supported by the observations that the maximum wavelength of 6-CF fluorescence shifts from 520 nm (6-CF in bound state) to 512 nm (6-CF in bulk solution) and that the shoulder at 540 nm in the 6-CF fluorescence spectrum disappears, beyond this concentration. The magnitude of the decrease in 6-CF fluorescence intensity just prior to saturation of the binding sites decreases with decreasing DADMAC mole percent. This is readily explained by decreased self-quenching of 6-CF since the local concentration of probe molecules along the polymer chain is less when there are fewer DADMAC groups on the polyelectrolyte. For the copolymers containing 8 and 21 mol % DADMAC, no decrease in the fluorescence intensity over the 6-CF concentration range studied was observed. Binding to the copolymers did, however, still occur, as revealed by spectral changes (see above).

Discussion

Electrostatic interactions are primarily responsible for the interaction of ionic probes with polyelectrolytes in solution.[7−9] Experiments where electrolyte (phosphate ions at 1 mM) was added to solutions containing 4-PSA or 6-CF already bound to PAH or PDADMAC caused the removal of the probe from the bound state to bulk solution. Addition of NaCl had a similar effect, but much higher electrolyte concentrations were required for probe removal. These observations point toward a competitive binding effect between the ions and probe, suggesting that the probes bind ionically to charged sites of the polyelectrolytes. To rule out hydrophobic interactions occurring between 4-PSA and polyelectrolytes, aliquots of unsubstituted pyrene in water[18] were added to aqueous solutions of PAH and PDADMAC. No interaction of pyrene with the polyelectrolytes was observed—the fluorescence properties of pyrene were the same in the absence and presence of PAH or PDADMAC.

The experimental data obtained reveal that the minimum of emission observed in the fluorescence versus fluorophore concentration curves corresponds to a situation of maximum filling or saturation of available binding sites on the polyelectrolytes. Evidence for this for 4-PSA comes from the monomer fluorescence intensity at the concentrations of maximum I_E/I_M (i.e., where the amount of probe bound is considered to be a maximum and the polyelectrolyte saturated with probe); the monomer intensity at this point is less than 1% of that for 4-PSA at the same concentration in the absence of polyelectrolyte. 6-CF residing in bulk solution can be identified by the shoulder at 540 nm in its fluorescence spectrum. The amount of 6-CF which is not bound to the polyelectrolyte prior to the minimum in the fluorescence intensity is so small that it is beyond detection by fluorescence measurements. Thus, the amount of probe in bulk solution at the concentration where saturation binding occurs (and prior to this range) is considered to be negligible. We can conclude that the probes bind with a high affinity and that the equilibrium between bound probe and that free in solution lies predominantly toward the bound state. These observations are consistent with the work of Tiera et al.,[6] where it was reported that when (1-pyrenylmethyl)trimethylammonium is added to a copolymer of poly(methallyl sulfonate−vinyl acetate) consisting of 19 mol % sodium methallyl sulfonate, all of the probe is localized at the water−copolymer interface; i.e., all of the probe is bound.

At saturation binding, the value of I_E/I_M (ca. 130) for 4-PSA with PAH is 2−3 orders of magnitude greater than that for 4-PSA when bound to PDADMAC ($I_E/I_M \sim 0.25$). This may reflect the more flexible nature of the PAH backbone compared to PDADMAC, as well as differences in the local structure (e.g., proximity, arrangement, and stereochemistry of binding sites) between PAH and PDADMAC. (A perfectly parallel orientation of the aromatic rings is not required for excimer formation and does not markedly influence the excimer emission intensity.[19]) On a local scale, PAH is more likely to adopt a more coiled conformation in solution than PDADMAC, which is a more rigid polymer; flexibility of the chain would enhance the formation of excimers through increased probe−probe interactions. The distance between charges in PDADMAC (7.5 ± 1.0 Å[20]) is greater than that between charges in PAH (5.8 ± 0.8 Å[20]) and may therefore account for the larger degree of monomer fluorescence observed for 4-PSA when bound to PDADMAC rather than PAH. This is also consistent with the absence of ground-state interactions of 4-PSA bound to PDADMAC suggested by the fluorescence excitation spectra (see earlier). A similar observation has been reported for the interaction of pyrenebutyric acid or 1-pyrenesulfonic acid with the cationic polyelectrolyte hexadimethrine bromide: neither excimers nor ground-state interaction of pyrene was observed with pyrenebutyric acid because of the larger distance between each charged group on the polyelectrolyte.[7]

Probe Behavior beyond Saturation Binding of Polyelectrolytes. At 6-CF concentrations just above the fluorescence minimum, the emission spectra show the reappearance of the shoulder at 540 nm, which is indicative of free (or unbound) 6-CF. The rate of 6-CF fluorescence intensity increase with 6-CF concentration (i.e., the slope) beyond saturation concentration (or

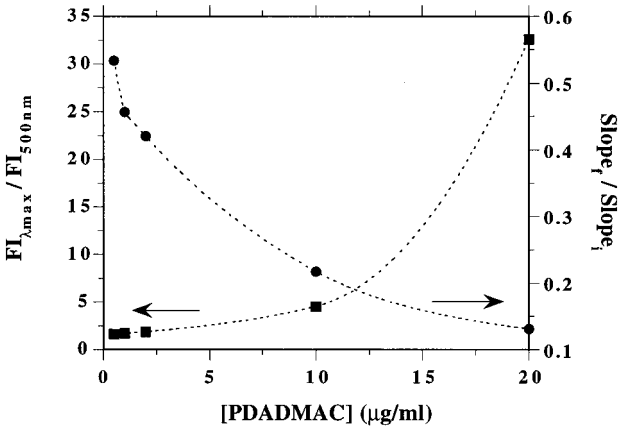

Figure 10. Plots of the ratio of fluorescence intensity taken at the maximum of 6-CF fluorescence to the 6-CF fluorescence intensity at 500 nm, and the ratio of the slope for 6-CF after saturation binding ($slope_f$) to the initial slope before the onset of quenching ($slope_i$), as a function of PDADMAC concentration. Excitation wavelength = 450 nm.

maximum quenching) is slightly lower than that in the absence of polyelectrolyte. If higher PDADMAC concentrations are used, the slope is even smaller. This relative decrease of the fluorescence slope with 6-CF concentration beyond the quenching maximum becomes systematically more pronounced with increasing total polyelectrolyte concentration (Figure 10). Although the binding stoichiometry (assessed at saturation binding) is not affected by PDADMAC concentration, $slope_f$ significantly decreases with increasing PDADMAC concentration. In parallel with this decrease in $slope_f$, the emission spectra become significantly broadened and red-shift with an increase in polyelectrolyte concentration. The relative degree of red-shift in the spectra is depicted in Figure 10, where the ratio of the fluorescence intensity taken at the maximum of fluorescence to the fluorescence intensity at 500 nm is plotted as a function of PDADMAC concentration. This observation indicates that resonance energy transfer and quenching of 6-CF occurs above the concentration of saturation binding. Further binding of 6-CF can be assumed not to occur beyond the saturation concentration since, if this were the case, the slope would be constant as both the 6-CF and polyelectrolyte concentrations increase proportionally. At saturation of binding sites about 50% of the total charged sites of the polyelectrolyte are compensated (see later). The fluorescence spectra suggest that the remaining polyelectrolyte charged sites still attract free 6-CF molecules but that they do not bind. This situation can be best described by the formation of a diffuse counterion layer by the excess free 6-CF molecules. This gives rise to a local concentration increase of free 6-CF near the polyelectrolyte chain, thus facilitating resonance energy transfer and quenching of the 6-CF forming the double layer. In contrast, the rate of fluorescence intensity increase with concentration for 4-PSA beyond saturation binding is only marginally less than that observed for 4-PSA in free solution. The slope beyond saturation binding for 4-PSA is less affected since there is a greater charge compensation of the polyelectrolyte (about 85%) when 4-PSA is bound (see later).

It is beyond the scope of this work to evaluate the mean distance between the probe in the counterion layer in order to obtain a quantitative description of energy transfer and quenching in this regime. Further, no analytical solutions for the case of charged cylinders providing either the potential as a function of distance from the polyelectrolyte or the number distribution of counterions are available. The particular cases of 6-CF and 4-PSA are complex because they represent asymmetric electrolytes with a large anion. Numerical simulation studies are required to obtain a solution for the probe distribution around the polyelectrolyte molecule. Nevertheless, the dependence of the Debye length on electrolyte concentration provides some information on the increasing effectiveness of quenching with increasing probe concentration. For example, for 6-CF, 1 μM yields a Debye length of 175 nm, while 10 μM gives 55 nm. Nonlinear effects must also be taken into account to understand the electrostatics around a charged cylinder.[21] These nonlinear effects lead to compression of the double layer, thus further enhancing the accumulation of counterions around the polyelectrolyte macroion.

Table 1. Number of Allylamine Hydrochloride (AH) or Diallyldimethylamine Chloride (DADMAC) Monomer Units per 4-PSA and 6-CF at Saturation Binding of PAH and PDADMAC[a]

	no. of monomer units/probe	
polyelectrolyte	4-PSA	6-CF
PAH	5.2 ± 0.2	3.7 ± 0.2
PDADMAC	4.8 ± 0.2	4.7 ± 0.2

[a] Calculated from the probe concentrations corresponding to saturation binding (see text for details). Values are the averages ± standard deviations for total polyelectrolyte concentrations ranging from 5 to 100 μg mL^{-1}.

Evaluation of 6-CF and 4-PSA Binding Stoichiometry at Saturation Binding. As detailed above, probe concentrations required to achieve the minimum of fluorescence for 4-PSA (same as the maximum of I_E/I_M) and 6-CF correspond to saturation of the polyelectrolyte chain by the binding probe. Hence, from these minima the limiting number of cationic monomers utilized by a probe can be determined. For 6-CF it is also possible to derive the point of saturation by evaluation of the emission spectra as a function of 6-CF concentration in the presence of polyelectrolyte. From the appearance of the shoulder at 540 nm in the fluorescence spectrum, the saturation concentration can be inferred. However, the accuracy of the concentration determined in this way is smaller than that obtained by evaluation of the binding stoichiometry from the minima of the fluorescence versus probe concentration curves. Nevertheless, this method at least allows the determination of the binding stoichiometry for 6-CF for low DADMAC contents in the DADMAC−AAM copolymers where a fluorescence minimum is not discernible in the experimental data.

The extent of probe binding to the polyelectrolytes is expressed as the ratio of the number of monomer units in the polyelectrolytes to each probe molecule bound. These values are given in Table 1 for PAH and PDADMAC. There are approximately 5 allylamine hydrochloride (AH) or DADMAC monomers for each 4-PSA molecule, 3.7 for each 6-CF molecule with PAH, and 4.7 for each 6-CF with PDADMAC, at saturation binding conditions.

Figure 11 shows the DADMAC monomer to probe ratio as a function of the DADMAC content in the DADMAC−AAM copolymer. The data for the homopolymer (100%) are also shown. The DADMAC monomer to 4-PSA ratio is approximately 5 and remains

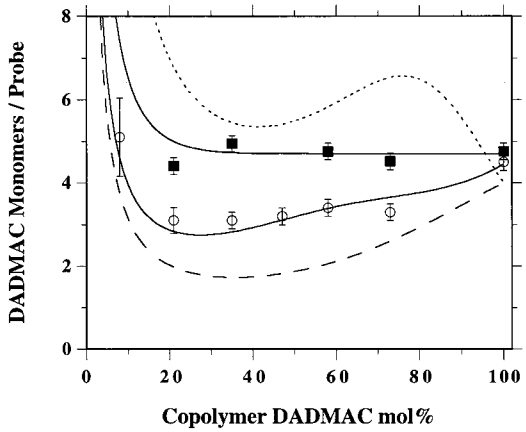

Figure 11. Number of DADMAC monomer units/probe for 4-PSA (squares) and 6-CF (circles) as a function of DADMAC mole percent in the copolymer. The experimental data for the homopolymer (PDADMAC, 100%) are also shown. Values are determined from the probe concentrations corresponding to the maximum in I_E/I_M for 4-PSA (Figure 8) or the minimum 6-CF fluorescence intensity at saturation binding (Figure 9). The solid curves are theoretical best fits to the data, while the dotted and dashed curves represent two limiting cases of the theoretical model for the binding stoichiometry. The theoretical curves were generated using eqs 1−4 given in the text.

essentially constant over the DADMAC content range 21−100 mol %. The DADMAC to 6-CF monomer ratio, however, decreases from a value of 4.7 in the case of the homopolymer to a value of approximately 3 at 21 mol % DADMAC. For 8 mol % DADMAC content, an increase in this ratio to 5.1 was derived from the analysis of the corresponding fluorescence spectra.

The difference in the observed DADMAC monomer to probe ratios for 6-CF and 4-PSA is significant. First, it is obvious that the 6-CF molecules bound do not fully compensate the charges on the polyelectrolyte chain. For example, for 100 mol % DADMAC (i.e., PDADMAC), half of the charges are equalized by the two carboxylic acid groups of 6-CF. This has important consequences for the behavior of the fluorescence concentration curves beyond saturation binding (see earlier). The ratio of 4.7 (mean value of the data) observed in the 4-PSA/DADMAC−AAM system indicates that approximately 85% of the DADMAC charges in the copolymer are electrostatically compensated by bound 4-PSA.

Analysis of the DADMAC monomer to probe ratio data provides information on the binding stoichiometry. In view of the current lack of a molecular picture on the binding process (which, in principle, can be obtained by means of molecular simulations), simple combinatorial mathematics can be applied to investigate the various possibilities of binding. Such an investigation prior to simulation studies is particularly useful since a number of unlikely situations can be excluded from the otherwise extremely time-consuming simulation procedures. We begin with the simplest case of assuming that 6-CF is capable of only binding to a pair of DADMAC sites located at a fixed distance apart. The concentration of such "paired sites" should decrease with decreasing DADMAC content as α^2 where α denotes the probability that a given site in the random DADMAC−AAM copolymer is DADMAC. α ranges from 0 to 1, with 1 corresponding to the DADMAC homopolymer. From these considerations it follows that the theoretical monomer to probe ratio should reach a value of $4/\alpha^2 = 91$ for 21 mol % DADMAC content if 4 corresponds to the homopolymer case. Such a dependence of the bound amount on the DADMAC content is in striking disagreement with the experimental data, which show only a slight decrease of the monomer to probe ratio in the case of 6-CF over the range 21−100 mol % DADMAC. In addition, the pair binding notion cannot explain the experimental value of about 4 for 100 mol % DADMAC. The ratio should be 2, assuming that both sites of the probe are bound to a single monomer charged site of DADMAC and that no other sterical constraints apply. Hence, more complex mechanisms need to be considered to explain why the binding of 6-CF increases instead of decreasing with DADMAC content. It is assumed that a single bound 6-CF molecule is capable of sterically occupying 4 DADMAC monomers, thus preventing binding of another 6-CF molecule to the remaining two sites unused by the first molecule. Thus, we identify a sequence of 4 DADMAC monomers as a binding site. Since 2 DADMAC monomers remain unused, it is straightforward to assume that both 3 monomers in a total of 4, and 2 in 4 will qualify as binding sites for 6-CF (in a sequence of 4 monomers). We further assume that even only 1 DADMAC site in a sequence of 4 represents a potential binding site. The theoretical DADMAC monomer to 6-CF ratio, $f(\alpha)$, can thus be written as

$$f(\alpha) = \left[\frac{\alpha^4}{4} + \frac{4\alpha^3(1-\alpha)}{3} + \frac{6\alpha^2(1-\alpha)^2}{2} + 4\alpha(1-\alpha)^3\right]^{-1} \quad (1)$$

The Appendix provides details of the derivation of this equation. Values generated from eq 1 are displayed in Figure 11 (lower dashed curve). Although the trend provided by eq 1 is in qualitative agreement with the experimental data, the amount of bound 6-CF is overestimated for the intermediate DADMAC content region. An alternative suggestion for the nature of binding sites, with the inherent trend of less 6-CF bound, can be derived if we additionally consider the arrangement of the DADMAC groups in a sequence of 4 monomers. If for the case of small and intermediate DADMAC contents a DADMAC monomer is at position 1 or 4, respectively, and at least one of the monomers 2 and 3 is made up by AAM, it is possible that as a result of having further DADMAC at positions −1 and 0, or 5 and 6, respectively, the binding of 6-CF occurs preferentially "over the border" of a randomly selected sequence of 4 monomers. To exclude this possibility, which is brought about by the long-range electrostatic attractive interaction of the DADMAC charges with those of 6-CF, we terminate every qualifying binding site except for the situation of 4 DADMAC monomers in a row with 1 uncharged monomer. The theoretical monomer to 6-CF ratio including this additional requirement becomes (see Appendix)

$$f(\alpha) = \left[\frac{\alpha^4}{4} + \frac{\alpha^3(1-\alpha)^2}{3} + \frac{\alpha^2(1-\alpha)^2}{2} + \alpha(1-\alpha)^2\right]^{-1} \quad (2)$$

The upper dotted curve in Figure 11 represents data generated from eq 2. Clearly, eq 2 underestimates the binding capacity of the random copolymer chain. Equations 1 and 2, however, may represent two limiting cases of the theoretical model for the binding stoichiometry. The experimental data fall in between these two limits.

Hence, eq 1 was modified to reach agreement with the experimental data. Surprisingly, very few changes were introduced into eq 1 to obtain coincidence of model predictions and experimental data. First, the contribution of the third term in eq 1 was reduced by 50%, and a single DADMAC site was taken as a binding site only in the instance that not 1 but 2 uncharged monomers were terminating the DADMAC on either side. Additionally, a common probability factor of 0.9 was introduced to adjust the overall height of the theoretical curves. Equation 3 provides the final result of these modifications (see Appendix):

$$f(\alpha) = \left[0.9\left[\frac{\alpha^4}{4} + \frac{4\alpha^3(1-\alpha)}{3} + \frac{3\alpha^2(1-\alpha)^2}{2} + 4\alpha(1-\alpha)^4\right]\right]^{-1} \quad (3)$$

Although it is speculative to discuss the molecular nature of the changes introduced since we do not have a picture of the topological arrangement of 6-CF bound to the chain, replacing the factor 6 in the third term of eq 1 by 3 can be readily explained by assuming that the 2 DADMAC in 4 monomers have to appear at the same side of the chain to qualify as a binding site. The necessity of termination of a single DADMAC monomer with 2 instead of 1 uncharged monomer is straightforward since otherwise adjacent groups of DADMAC monomers would effectively compete for the binding 6-CF. The factor of 0.9 is related to the fact that on average 10% of 3 monomers may form a binding site; however, the majority of binding sites are brought about by 4 monomers. The nature of this sterical factor cannot be further explored without entering into molecular details.

The constant DADMAC to 4-PSA ratio with varying DADMAC content in the copolymer cannot be explained by a combinatorial model based on the assumption of the 4 sulfonate groups of 4-PSA binding to a group of adjacent DADMAC groups extending over the dimensions of 4-PSA. It has to be concluded that each sulfonate group binds individually to a DADMAC site located almost anywhere including the possibility of being a member of another copolymer molecule. This assumption implies that 4-PSA complexes the copolymer chain(s), with intramolecular and intermolecular cross-linking taking place. Such complexing may explain the strong binding observed for 4-PSA with the polyelectrolytes. Intramolecular cross-linking may result in loop formation, while intermolecular cross-linking may produce chain dimers with a largely parallel orientation. The latter possibility seems to be most probable for the higher DADMAC content copolymers and for the homopolymer. The corresponding dependence of the DADMAC to 4-PSA ratio taken as a function of the DADMAC content can be written as (see Appendix):

$$f(\alpha) = \frac{4.7}{1-(1-\alpha)^n} \quad (4)$$

The denominator in eq 4 describes the probability of finding at least 1 DADMAC monomer in a sequence of n monomers. The corresponding curve for the 4-PSA data in Figure 11 was generated with $n = 12$. This value suggests that the spacing of the sulfonate−DADMAC pairs formed by the binding of 1 4-PSA molecule can be separated by at least 12 random monomers. This value of n particularly applies for the 21 mol % DADMAC copolymer. At higher DADMAC contents more adjacent DADMAC monomers will be utilized as binding entities; smaller n values ($n \geq 5$) for eq 4 also describe the data in the 35−100 mol % DADMAC content range rather well. The value of 4.7 is again related to topological constraints, meaning that at the higher DADMAC contents 1 4-PSA molecule will occupy on average slightly more than 4 DADMAC sites. At lower DADMAC contents 4.7 can also be understood as a factor accounting for the fact that, in inter- and intramolecular complexes formed by the interaction of 4-PSA with various DADMAC sites, some DADMAC sites are not accessible for further binding. Additional strong support for the notion of 4-PSA-induced complexation comes from the observation that the excimer to monomer intensity ratio increases with increasing polymer concentration.

Interpretation of Probe Fluorescence−Concentration Binding Curves up to Saturation Binding. (a) 6-CF. Figure 9 shows that the extent of 6-CF quenching, as assessed by the depth of the minimum of fluorescence intensity, decreases with decreasing DADMAC content. This minimum also shifts to lower 6-CF concentrations with decreasing DADMAC mole percent in the copolymer. This can be primarily interpreted as being a result of the lower net DADMAC content. For 21 mol % DADMAC content, no minimum of fluorescence is found. Instead, a transient decrease of the slope indicates the presence of some residual quenching. For the 8 mol % DADMAC copolymer, the fluorescence concentration curves show no indication of quenching. The 6-CF curves are very similar in shape in the initial (0−3 μM) concentration range. These two observations indicate the presence of at least two independent processes responsible for quenching. At lower 6-CF concentrations, that is, prior to and below the maximum of fluorescence, the DADMAC content does not significantly influence the degree of quenching. At higher 6-CF concentrations, however, the number of available binding sites determines the depth and position of the minimum of fluorescence. As will be shown below, the occurrence of the minimum is due to a cooperative effect becoming more and more pronounced if the number of bound probes increases.

Fluorescence spectra measured for the 6-CF/DADMAC−AAM systems near the fluorescence minimum show significant red-shifts and broadening. Resonance energy transfer between bound 6-CF probes is therefore a major process to be considered at 6-CF concentrations close to the minimum. The absence of a shoulder in all of the 6-CF fluorescence spectra recorded for 6-CF concentrations prior to the minimum in fluorescence indicates that the binding constant of 6-CF to the copolymer is considerably high. Thus, free 6-CF probes in solution do not contribute to the fluorescence until after the minimum.

To quantitatively explain the probe quenching behavior induced by binding to the polyelectrolytes, we further explore the probability approach applied for evaluation of the binding stoichiometry. As discussed earlier, the slope of the fluorescence intensity versus 6-CF concentration curves after the fluorescence minimum is influenced by 6-CF forming a double layer around the partially charged polyelectrolytes. The model outlined below is, therefore, primarily designed for describing the concentration range prior to and

around the fluorescence minimum. First, we describe the equilibrium distribution of free probes, F_{free}, and probes bound to a site *S*, FS, by a single reaction mechanism

$$F_{free} + S \rightleftarrows FS \tag{5}$$

where *S* denotes the binding sites of the polyelectrolyte chain, the nature of which has been specified when discussing the binding stoichiometry of 6-CF. Hence, the concentrations of bound, c_b, and free probe, c_f, are provided by the solution to the following equations:

$$K = \frac{c_b}{c_m c_f} \tag{6}$$

$$c_f + c_b = c_0 \tag{7}$$

$$c_m + c_b = f(\alpha)^{-1} c_{m0} \tag{8}$$

where *K* is the binding constant, c_m denotes the concentration of occupied binding sites, c_{m0} is the total concentration of DADMAC monomers, and $f(\alpha)^{-1}$ relates the binding site concentration to that of DADMAC.

The solution of eqs 6−8 with regard to free and bound probe distributions is given by

$$c_b = \frac{1}{2}\left[c_0 + f(\alpha)^{-1}c_{m0} + \frac{1}{K} - \left[\left(c_0 + f(\alpha)^{-1}c_{m0} + \frac{1}{K}\right)^2 - 4f(\alpha)^{-1}c_0 c_{m0}\right]^{1/2}\right] \tag{9}$$

$$c_f = \frac{1}{2}\left[c_0 - f(\alpha)^{-1}c_{m0} - \frac{1}{K} + \left[\left(c_0 + f(\alpha)^{-1}c_{m0} + \frac{1}{K}\right)^2 - 4f(\alpha)^{-1}c_0 c_{m0}\right]^{1/2}\right] \tag{10}$$

The probability that a bound reference probe does not quench by means of interaction with a molecule bound to a selected site within its fluorescence lifetime will be derived next. Quenching is possible only if the second site is occupied by another probe molecule. This probability is given by the ratio of bound probe divided by the total number of available sites. Second, during the fluorescence lifetime of the probe, a transient dimer has to be formed in order to produce quenching. Whether a transient dimer may be formed depends on both the distance between the two molecules and the conformational flexibility of the polyelectrolyte. We denote the probability that quenching occurs between two probes at the reference and the selected occupied site during the probe fluorescence lifetime as f_i, where *i* denotes the position of the selected site with regard to the reference. Hence, the probability p_i that a probe does *not* quench the reference molecule is given by

$$p_i = 1 - f_i\left(\frac{c_b}{f(\alpha)^{-1}c_{m0}}\right) \tag{11}$$

The total probability that the reference probe emits monomer fluorescence *P* is

$$P = \prod_{i=1}^{\infty} p_i \tag{12}$$

We now examine the nature of the coefficients f_i. Since neither the molecular arrangement nor the flexibility and motion of the polyelectrolyte with its bound probes is precisely known, the following analysis is restricted to probability considerations. For simplicity we assume that there are two types of sites. (1) Probes bound to sites of type 1 may form dimers with the reference molecule during its fluorescence lifetime. We denote *j* as the number of sites of type 1. *j* should be small given the topological constraints of the polyelectrolyte chain. The linear symmetry of the polyelectrolyte chain requires *j* to be an even integer. (2) Probes bound to type 2 sites are too far from the reference molecule to directly form dimers. They may, however, transfer energy to neighboring sites by means of a resonance mechanism. Such energy channeling may proceed further until the transferred energy encounters a quenching dimer. The critical distance for 6-CF Förster energy transfer is 5.1 nm.[13] This is considerably larger than the spacing between binding sites in the homopolymer which is on the order of 1−2 nm. Thus, a resonance energy-transfer mechanism should, in principle, be capable of transferring energy over sites not occupied by probes. These assumptions allow derivation of a relationship between f_i and the bound probe concentration, as well as the DADMAC content:

$$f_i = k_{di}g(\alpha) \qquad i \le j \text{ (type 1)} \tag{13}$$

$$f_i = k_{ri}g(\alpha)^{i/2}\left(\frac{c_b}{f(\alpha)^{-1}c_{m0}}\right)^{(i-1)/2} \qquad i > j \text{ (type 2)} \tag{14}$$

where k_{di} and k_{ri} are probability coefficients describing the efficiency of quenching and transfer, respectively. $k_{di} = 1$ if a quenching dimer is always formed between the reference molecule and the second probe occupying the site number *i* during the fluorescence lifetime. $g(\alpha)$ denotes the probability that a particular sequence of monomers constitutes a binding site *i*. Arriving at eq 14, it was assumed that at least half of the sequences are a potential binding site and are occupied by a probe to provide conditions for resonance energy transfer to occur. The probability $g(\alpha)$ is given by (cf. eq 3):

$$g(\alpha) = 1 - [(1-\alpha)^4 + 2\alpha^2(1-\alpha)^2 + 2\alpha(1-\alpha)^4] \tag{15}$$

k_{ri} should decrease with *i* since longer sequences of bound probes should be equally spaced to take part in the resonance energy-transfer mechanism. It should be noted that eqs 11, 12, and 14 describe a highly cooperative effect, which is largely responsible for the decrease of fluorescence prior to the minimum. Finally, the total monomer fluorescence intensity FI is found as the sum of the fluorescence of bound and free monomers:

$$FI = q_b P c_b + q_f c_f \tag{16}$$

where q_b and q_f are the quantum yields for the bound and free states of the probe, respectively.

The curves obtained from the above model for the 6-CF/DADMAC−AAM and PDADMAC systems provide excellent fits to the experimental data (dashed curves, Figure 9). Next we will show that only a few parameters are needed for the fit and that the values obtained for the parameters are reasonable. Experimentally accessible parameters for the theoretical curves are the two increments of fluorescence at the lowest 6-CF concentrations and at those well beyond the fluorescence

minimum. These two parameters essentially represent the quantum yields q_b and q_f in eq 16. q_f is smaller than q_b as a result of the concentration increase in the diffuse part of the double layer formed around the 6-CF-saturated, but still partially charged, polyelectrolyte chain.

Three parameters, K, k_{di}, and k_{ri}, were varied to obtain best fits to the experimental data in the region prior to saturation binding. First, the binding constant K only determines the sharpness of the minimum of fluorescence but has no influence on the fluorescence intensity in the concentration range prior to the minimum. A binding constant of 2.5×10^7 M^{-1} described the sharpness sufficiently well. While the various sites corresponding to different numbers of DADMAC monomers involved may, in principle, have different binding constants, they do not affect the theoretical fluorescence versus 6-CF concentration curves prior to the minimum because the binding constants have to be taken large enough to ensure the absence of free 6-CF until the minimum is reached. (This is in agreement with the experimental data.) Second, the probability of formation of a dimer from adjacently bound 6-CF molecules (k_{di}) with the subsequent quenching of the excited state of one of the molecules is small in the cases of the DADMAC−AAM copolymers and PDADMAC. Attempts to describe the experimental data with a larger probability of dimer formation to account for the minimum produced flat curves which did not display the steepness of the decrease in fluorescence before the minimum, nor did they produce the maximum fluorescence intensity at the required concentration range while giving the correct height of the fluorescence minimum. From these considerations it is clear that, in order to explain the fluorescence minimum, the transfer of energy is the major mechanism for the enhanced quenching. Equations 12 and 14 provide the necessary cooperativity expressed by the power law $P(c_b)$. These findings are in agreement with the shape of the emission spectra around the fluorescence minimum, where large broadening and red-shifts of the maximum of fluorescence by as much as 25 nm are observed. Such changes are characteristic of energy-transfer processes to lower energy states. As a result of these considerations together with an adjustment process of the observed theoretical curves, k_{di} was found to be 0.18 and k_{ri} equal to $2.25i^{-1}$ ($i \geq 3$). It was further established that only two binding sites are capable of forming a dimer with the reference site when occupied by a 6-CF molecule. It is straightforward to assume that these sites are in close proximity to the reference site. They may even represent the two neighbors on each site.

Since the two probabilities k_{di} and k_{ri} should, in principle, depend on the dynamics of the chain and on the orientation of the probes along the chain, it cannot be expected that they are constant if DADMAC monomers are replaced by AAM monomers, which is the case when decreasing the DADMAC content in the copolymer. For example, increasing the flexibility of the chain may result in an increase in k_{di}. It is also conceivable that the degree of binding itself influences the flexibility of the chain, because an increased amount of 6-CF bound to the DADMAC charges reduces the lateral repulsion along the chain, which in turn may lead to a decreased bending resistance. Therefore, it cannot be expected that two constant parameters will lead to theoretical curves describing every detail of the fluorescence versus 6-CF concentration dependency. Nevertheless, the agreement obtained using the above model is excellent when the same constants for all of the copolymers are used.

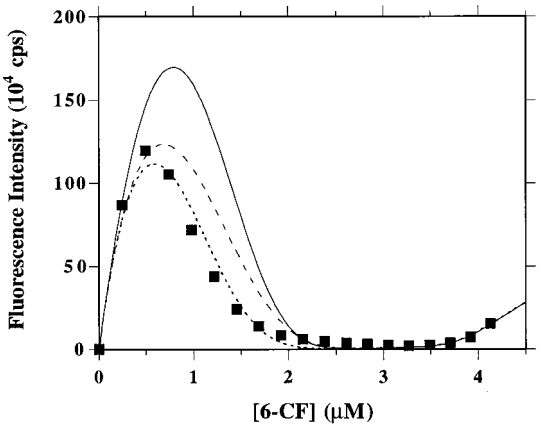

Figure 12. Fluorescence intensity as a function of concentration for 6-CF in the presence of 1.7 μg mL^{-1} PAH. Excitation wavelength = 450 nm. Lines: theoretical curves generated using the probability model detailed in the text; $K = 2 \times 10^8$ M^{-1}. Dotted and dashed curves: $k_{di} = k_{ri} = 1$ (for all values of i). Solid curve $k_{di} = 0.5$ (for all values of i). Dotted and solid curves: every fifth binding site is occupied by 6-CF to result in resonance energy transfer. Dashed curve: every third binding site is occupied by 6-CF to result in resonance energy transfer.

Figure 12 shows a typical example of the fluorescence intensity of 6-CF when PAH is used as the binding polyelectrolyte. There are two major differences compared with the 6-CF/DADMAC−AAM or PDADMAC interactions. First, the extent of quenching is close to 100% and occurs over a wide range of 6-CF concentrations. Second, the maximum of fluorescence occurs at a lower 6-CF concentration. Both observations indicate that the interaction of 6-CF with PAH leads to significantly more quenching compared with the 6-CF/PDADMAC interaction. Broadening of the emission spectrum and a red-shift were also observed under the conditions where the fluorescence minimum occurs.

When it was attempted to describe the 6-CF quenching curve data using the above model, both probability coefficients k_{di} and k_{ri} needed to be increased to account for the high quenching capacity of 6-CF when bound to PAH compared to PDADMAC. Furthermore, it was necessary to increase the number of sites capable of forming dimers with a bound reference 6-CF molecule to 4, rather than 2, as is the case for PDADMAC. These changes yielded broad fluorescence curves around the minima, but the maximum was not sufficiently shifted toward lower 6-CF concentrations. As illustrated by the curves (Figure 12), a further shift of the maximum of fluorescence is possible when it is assumed that, on average, not every second but only every fifth site has to be occupied by a 6-CF molecule to ensure efficient transfer of energy to a dimer trap. These findings are in good agreement with the notion that PAH is a more flexible polyelectrolyte than PDADMAC. The large flexibility of the PAH chain allows both high rotational and bending motion of the chain during the probe fluorescence lifetime. It is thus possible that, during the lifetime of fluorescence, appropriate transient conformations of the chain occur, producing more favorable conditions for increased energy transfer of neighboring but separated 6-CF molecules. The mean distance

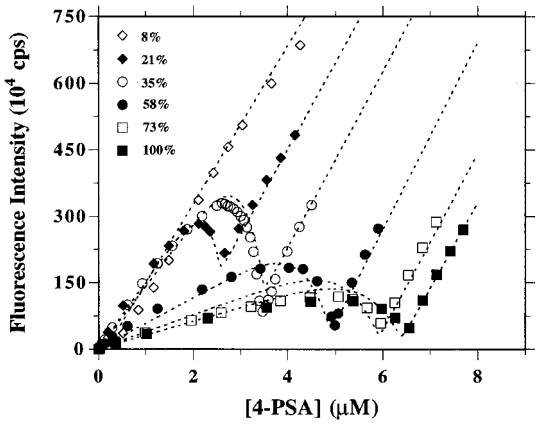

Figure 13. Fluorescence intensity as a function of concentration for 4-PSA in the presence of 5 μg mL^{-1} DADMAC−AAM copolymers with various charge densities. The DADMAC contents in the copolymers are 8, 21, 35, 58, and 73 mol %. The experimental data for the homopolymer (PDADMAC, 100%) are also shown. Excitation wavelength = 350 nm. The curves are theoretical fits to the experimental data (see text for details). $K = 10^{10}$ M^{-1}, $k_{di} = 0.6$, $k_{ri} = 0.9$ for $i = 3$, and $k_{ri} = 0$ for $i > 3$.

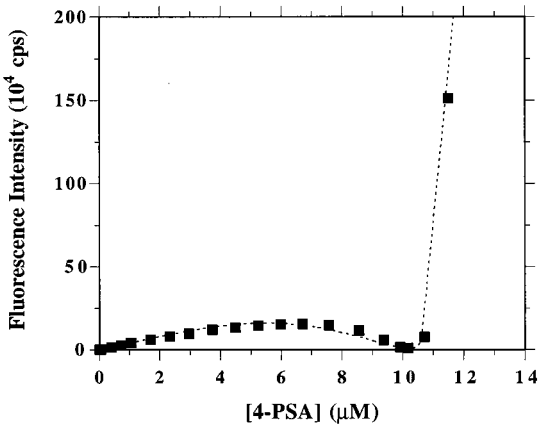

Figure 14. Fluorescence intensity as a function of concentration for 4-PSA in the presence of 5 μg mL^{-1} PAH. Excitation wavelength = 350 nm. The curve is a theoretical fit generated using the probability model detailed in the text; $K = 10^{10}$ M^{-1}, $k_{di} = 0.88$, $k_{ri} = 1$ for $i = 3$, and $k_{ri} = 0$ for $i > 3$, $n = 2$.

between 5 binding sites on a PAH chain is 5 × 4.7 × 0.3 = 7.0 nm (mean occupancy of binding sites by 6-CF × mean number of used binding sites × projection of mean distance of monomers onto the chain axis), assuming a fully extended chain. This distance is only slightly larger than the Förster distance of 5.1 nm for 6-CF.[13] Thus, also taking into account that any bending deformation would reduce this distance, it is probable that 5 binding sites for the mean separation qualifying for a Förster mechanism of transfer (obtained from fitting the experimental data) is the upper limit for resonance energy transfer to occur. It should be noted that the "stiffness" of the polymer may change upon binding of 6-CF. Although no molecular model for the interaction of 6-CF with PAH, obtained by stereochemical considerations or simulation, has been proposed so far, it is conceivable that the relatively large 6-CF molecules compared with the dimensions of a monomer unit may significantly reduce the freedom of rotational and bending motion of the chain. This might explain why the theoretical fits always give 100% quenching in the minimum region, whereas the experimental data show some residual fluorescence around the broad minimum. It is further worth noting that the theoretical fits indicate a 10-fold stronger binding of 6-CF to PAH, compared with 6-CF binding to PDADMAC. This again could be a result of the larger flexibility of PAH, allowing for better adaptation of the binding sites to the molecular shape of 6-CF.

(b) 4-PSA. The monomer fluorescence intensity of 4-PSA is plotted as a function of the 4-PSA concentration for the series of DADMAC−AAM copolymers (including PDADMAC) and PAH in Figures 13 and 14, respectively. Particularly at higher DADMAC contents and always with PAH, it is evident that even at the lowest 4-PSA concentrations studied the monomer fluorescence increment with concentration is much smaller than that for 4-PSA in solution in the absence of polyelectrolyte. At the same time, even the lowest 4-PSA concentrations used also yield excimer fluorescence. Only when the DADMAC content is 35 mol % or less does the initial rate of increase of monomer fluorescence equal that of free 4-PSA in solution at low 4-PSA concentrations. This behavior cannot be explained by an independent binding of the individual 4-PSA molecules, since at low 4-PSA concentrations the majority of bound 4-PSA undergoes quenching and/or excimer formation. Therefore, it can be concluded that binding of 4-PSA occurs preferentially next to a bound 4-PSA molecule, provided the DADMAC content of the copolymer is high enough. Two explanations can be readily given for this behavior, which is qualitatively different from that of 6-CF. First, the mutual attraction of the aromatic moieties of 4-PSA molecules may be sufficiently large to facilitate a stacking interaction of 4-PSA. Second, the creation of a local concentration enhancement of binding DADMAC sites by a bound 4-PSA may also cause further 4-PSA binding in stacks. If binding of 4-PSA is accompanied by intra- or intermolecular cross-linking next to another bound 4-PSA, more DADMAC sites (from two parts of a chain or from two chains) may become available for the binding of a second 4-PSA molecule. This suggested mechanism can be best described as a "zipper" mechanism. The observation that the excimer fluorescence needs several minutes to reach a maximum after addition of further 4-PSA to the sample is in full agreement with this suggested hypothesis of binding. It may take some time given the strong binding of 4-PSA for the bound 4-PSA to redistribute from pairs or stacks of molecules.

Another characteristic feature of the 4-PSA monomer fluorescence−concentration curves is the relatively sharp bend toward low fluorescence values close to the point of saturation of the DADMAC−AAM or PDADMAC chain. This "turnover point" occurs at a higher concentration range compared with that observed for 6-CF. The 6-CF fluorescence "turnover" may be explained mainly by resonance energy transfer. Since for 4-PSA resonance energy transfer is not likely to occur, the large negative slope just before the fluorescence minimum is reached indicates a highly cooperative effect. While at low and medium 4-PSA bound amounts (compared with saturation binding) many zippers may grow independently of one other, closer to saturation binding, interaction of these individual stacks or pairs must take place. If the fluorescence prior to the downward bend is partly attributed to "end effects" of the stacks or pairs, the reorganization taking place will increase with increased filling of sites and will lead to a pronounced decrease of the monomer fluorescence intensity.

The above qualitative considerations are now discussed in quantitative terms by applying the suggested probability model to the interaction of 4-PSA with the DADMAC−AAM copolymer (and PDADMAC) and PAH. The adopted pair or stack model of binding requires the removal of the concentration dependence of the monomer fluorescence probability of site number i. In the idealized case a neighboring site to the reference site is always occupied by another 4-PSA molecule, regardless of the bound amount. The fact that the chain is partly empty until saturation is reached is taken into account by the first term of eq 16, where the total monomer fluorescence is proportional to c_b. Equation 11 now becomes

$$p_i = 1 - f_i \tag{17}$$

where f_i consists of two factors: first, the coefficient k_{di} introduced earlier which describes the probability of quenching between an occupied site i by 4-PSA and the reference molecule and, second, the probability that a neighboring site qualifies for binding. The necessary criteria for binding as a neighbor capable of self-quenching or excimer formation are not known a priori; therefore, reasonable assumptions within the framework of the probability approach have to be made to bring into coincidence the experimental data and the theoretical curves. It is clear that if next to a bound 4-PSA molecule no DADMAC sites are present in the copolymer, a pair of 4-PSA molecules cannot be formed. Since the initial slopes of the 4-PSA fluorescence versus concentration curves for 58 and 73 mol % DADMAC−AAM copolymers and PDADMAC (100%) shown in Figure 13 are significantly smaller than the initial slope for free 4-PSA in solution whereas those of 35 mol % and lower DADMAC content approach that of free 4-PSA in solution, a reasonable suggestion is that, for example, 2 out of 4 sites next to a bound 4-PSA must be present to form a quenching pair. The probability for this case is given by

$$g_i(\alpha) = \alpha^4 + 4\alpha^3(1-\alpha) + 6\alpha^2(1-\alpha)^2 \qquad i \le 2 \tag{18}$$

i has been taken as less than or equal to 2 to account for the linear symmetry of the polyelectrolyte chain. Equations 17 and 18 describe the regions of low and medium concentrations of bound 4-PSA. The sharp decrease of fluorescence at 4-PSA concentrations close to chain saturation has to take into account the cooperativity brought about by sites further apart when the individual pairs or stacks grow together. Since detailed mechanisms about the ordering are not available, nor is the molecular architecture of binding, the description of cooperativity has to be on a phenomenological level. It is a priori clear that f_i for $i > 2$ must be connected by means of a power law to the exponent n with the relative bound amount. It is further obvious that if no DADMAC sites are available, contact of the individual stacks upon filling cannot occur. These rather qualitative considerations lead to the following expression for f_i with $i > 2$:

$$f_i = \left[\frac{c_b}{f(\alpha)^{-1} c_{m0}}\right]^n [1 - (1-\alpha)^4] \tag{19}$$

The theoretical curves generated from eqs 17−19 and eqs 12 and 16 are compared with the experimental data in Figures 13 and 14. Good coincidence of the theory and experimental data is obtained when n is taken to equal 7 and summations are carried out only over three indices, which is equivalent of allowing only neighboring interactions and no long-range transfer of energy or coupling. k_{di} was found to be equal to 0.6, while k_{ri} ($i = 3$) equaled 0.9. The value of 7 for n is an indication of an extraordinarily high cooperativity. Despite the fact that the model cannot take into account the molecular architecture of the mutual binding process, the rather good description of all of the important features of the experimental data, such as the sharp minimum, its height, high cooperativity, and the initially small slope of the higher DADMAC content copolymers, indicates that the general understanding of the process for 4-PSA binding to DADMAC−AAM copolymers and PDADMAC is correct.

The above model also well-described the 4-PSA/PAH binding and subsequent quenching when the k_{ri} and k_{di} values were taken to be larger, in agreement with the higher flexibility of the PAH chain (Figure 14). The cooperativity was significantly smaller ($n = 2$), which can also be interpreted as a result of the more flexible nature of PAH. The rather stiff nature of 4-PSA may allow it to be "wrapped" by the flexible PAH chains. When the individual stacks grow together, no large-scale conformational changes of the PAH chain are required.

Conclusions

It has been demonstrated that the binding topology of 4-PSA and 6-CF is qualitatively and quantitatively different for the polyelectrolytes studied. 4-PSA complexes the cationic polyelectrolyte chains, whereas 6-CF binds to a sequence of DADMAC monomers located on the same chain in close proximity. This difference in behavior is attributed to the weaker binding of 6-CF compared with that of 4-PSA; 6-CF contains *2* weak carboxylic acid groups, while 4-PSA has *4* strongly acidic sulfonate groups per molecule available for binding. This difference is also most probably responsible for the smaller capability of 6-CF (compared with 4-PSA) to compensate the cationic groups by localized electrostatic-facilitated binding. Evaluation of the probe fluorescence−concentration binding curves, based on a probability model of probe binding and quenching efficiency, enabled determination of the connection between quenching efficiency and polyelectrolyte molecule spatial motion. The derived probability model was found to provide both good qualitative and quantitative agreement with the fluorescence quenching data for 4-PSA and 6-CF as a result of their binding to the cationic polyelectrolytes studied. Further studies may exploit findings to study the flexibility of polyelectrolytes by means of the static and dynamic fluorescence of the bound probes. The 4-PSA−polyelectrolyte interactions are a promising way of constructing ordered intermolecular complexes by the self-assembly of cross-linking compounds with a high symmetry and rigidity of their binding entities. Systematic investigations of the fluorescence behavior of probe molecules interacting with polyelectrolytes beyond the saturation range may also serve as a new means to investigate the double-layer properties around charged molecular cylinders. This could lead to valuable contributions toward the understanding of polyelectrolyte behavior and interactions in aqueous systems. In a subsequent publication,[22] the anionic probes used in this study will be

employed to characterize ultrathin multilayer polyelectrolyte films of PAH and PDADMAC (alternating with PSS) in order to arrive at a better understanding of the electrostatic interactions between the polyelectrolytes in the films.

Acknowledgment. F.C. acknowledges the Alexander von Humboldt Foundation for a Research Fellowship.

Appendix

Derivation of Equations 1−4. A DADMAC monomer is denoted as a and an AAM monomer as b. α is the probability of finding a DADMAC monomer at a specified position in the copolymer chain. To obtain eq 1, it is assumed that there is at least 1 a in a sequence of 4 arbitrary monomers to form a binding site for 6-CF in the random DADMAC−AAM copolymer (assumption 1). The probability for the sequence aaaa to occur is α^4; any of the 4 possible sequences with only 1 b in 4 monomers (for example, abaa) has the probability $\alpha^3(1 - \alpha)$. There are 6 possibilities to combine 2 b with 2 a (for example, abab): each one has the probability $\alpha^2(1 - \alpha)^2$. Finally, 4 sequences with only 1 a, each with the probability $\alpha(1 - \alpha)^3$, provide all possible binding site topologies within the framework of assumption 1. Next we express the concentration of each of the above 15 configurations as a function of the total DADMAC monomer concentration, c_{m0}:

$$c_{aaaa} = \alpha^4 c_{m0}/4, \quad c_{baaa} = \alpha^3(1 - \alpha)c_{m0}/3 \ldots \quad \text{(A1)}$$

The sum of all 15 equations in (A1) provides the total binding site concentration, from which eq 1 directly follows, describing the theoretical DADMAC monomer to 6-CF ratio, $f(\alpha)$, at binding saturation conditions.

Equation 2 was derived with the assumption that a binding site for 6-CF contains 1−4 a with a terminating b at both ends except in the case of aaaa, where no termination is required (assumption 2). Hence, the following sequences qualify for 6-CF binding: aaaa, baaab, baab, bab. The derivation of eq 2 is analogous to that of eq 1.

Equation 3 was obtained as a result of fitting the experimental data by varying the binding site assumptions (see the main text). In particular, eq 3 identifies the following binding topologies as potential 6-CF binding sites: aaaa, 4 sequences of a, a, a, b in arbitrary arrangement, only 3 sequences of the 6 possible sequences consisting of a, a, b, b, and finally the situation b, a, b, b, b, where, however, only 4 out of the possible 5 sequences are assumed to be utilized by 6-CF.

It was assumed that 4-PSA complexes the DADMAC−AAM copolymer by binding with each group to a DADMAC monomer which can belong to a different section of the same chain or even to another polymer chain. In such a situation a defined site topology as a prerequisite for binding may not exist. However, if the spacing between the DADMAC monomers becomes too large, binding of 4-PSA may be difficult due to topological constraints. The probability of having a continuous sequence of n AAM monomers is given by $(1 - \alpha)^n$. Hence, the probability of having DADMAC monomers spaced by $n - 1$ or a smaller number of AAM monomers is given by $1 - (1 - \alpha)^n$.

References and Notes

(1) See, for example; Grätzel, M.; Thomas, J. K. In *Modern Fluorescence Spectroscopy*; Wehry, E. L., Ed.; Plenum: New York, 1976; Vol. 2. Zachariase, K. A.; Kozankiewicz, B.; Kühnle, W. In *Surfactants in Solution*; Mittal, K. L., Ed.; Plenum: New York, 1983. Winnik, M. A. In *Polymer Surfaces and Interfaces*; West, W. J., Munro, H. S., Eds.; Wiley: New York, 1987; pp 1−31. Almgren, M.; Grieser, F.; Thomas, J. K. *J. Am. Chem. Soc.* **1979**, *101*, 279. Atik, S. S.; Thomas, J. K. *J. Am. Chem. Soc.* **1982**, *104*, 5868. Bohorquez, M.; Patterson, L. K. *Langmuir* **1990**, *6*, 1739. Caruso, F.; Grieser, F.; Thistlethwaite, P. J.; Almgren, M. A.; Wistus, E.; Mukhtar, E. *J. Phys. Chem.* **1993**, *9*, 7364.
(2) For a review, see: Rangarajan, B.; Coons, L. S.; Scranton, A. B. *Biomaterials* **1996**, *17*, 649.
(3) Branham, K. D.; Shafer, G. S.; Hoyle, C. E.; McCormick, C. L. *Macromolecules* **1995**, *28*, 6175.
(4) Chu, D. Y.; Thomas, J. K. *Macromolecules* **1990**, *23*, 1059.
(5) Herkstroeter, W. G.; Martic, P. A.; Hartman, S. E.; Williams, J. L. R.; Farid, S. *J. Polym. Sci., Polym. Chem. Ed.* **1983**, *21*, 2473.
(6) Tiera, M. J.; Neumann, M. G.; Bertolitti, S. G.; Previtali, C. M. *J. Macromol. Sci., Pure Appl. Chem.* **1992**, *A29*, 689. Tiera, M. J.; Neumann, M. G.; Bertolitti, S. G.; Previtali, C. M. *J. Macromol. Sci., Pure Appl. Chem.* **1994**, *A31*, 439.
(7) Zimerman, O. E.; Cosa, J. J.; Previtali, C. M. *J. Macromol. Sci., Pure Appl. Chem.* **1994**, *A31*, 859.
(8) Hrdlovic, P.; Horinova, L.; Chmela, S. *Can. J. Chem.* **1995**, *73*, 1948.
(9) Becker, H. G. O.; Schütz, R.; Kuzmin, M. G.; Sadovsky, N. A.; Soboleva, I. V. *J. Prakt. Chem.* **1987**, *329*, 87. Becker, H. G. O.; Schütz, R.; Kuzmin, M. G.; Soboleva, I. V. *J. Prakt. Chem.* **1987**, *329*, 95.
(10) Turro, N. J.; Pierola, I. F. *Macromolecules* **1983**, *16*, 906.
(11) Turro, N. J.; Okubo, T.; Chung, C.-J.; Emert, J.; Catena, R. *J. Am. Chem. Soc.* **1982**, *104*, 4799.
(12) Haugland, R. P. In *Molecular Probes Handbook of Fluorescent Probes and Research Chemicals*, 6th ed.; Spenz, M. T. Z., Ed.; Molecular Probes: Eugene, OR, 1996; p 19.
(13) Chen, R.; Knutson, J. *Anal. Biochem.* **1988**, *172*, 61.
(14) Reid, R. F.; Soutar, I. *J. Polym. Sci., Polym. Phys. Ed.* **1978**, *16*, 231.
(15) Anderson, R. A.; Reid, R. F.; Soutar, I. *Eur. Polym. J.* **1979**, *15*, 925.
(16) Decher, G. *Science* **1997**, *277*, 1232. Decher, G.; Hong, J.-D. *Makromol. Chem., Macromol. Symp.* **1991**, *46*, 321.
(17) Brandt, F.; Dautzenberg, H.; Jaeger, W.; Hahn, M. *Angew. Makromol. Chem.* **1997**, *248*, 41.
(18) Pyrene is slightly soluble in water. See: Schwarz, F. P. *J. Chem. Eng. Data* **1977**, *22*, 273.
(19) Wang, Y. C.; Morawetz, H. *Makromol. Chem., Suppl.* **1975**, *1*, 283.
(20) Distances between the charged groups on the polyelectrolytes and those on the probes were determined by molecular dynamics simulations using the program DISCOVERY. The values for the polyelectrolytes are the averages for the isotactic and syndiotactic forms of PAH and PDADMAC.
(21) Kenneth, S. S. *Macroions in Solution and Colloidal Suspension*; VCH Publishers: New York, 1993; Chapter 5.
(22) Caruso, F.; Lichtenfeld, H.; Donath, E.; Möhwald, H. Submitted.

MA980538D